Research On Prediction And Estimation Of Power Electronic Equipment Operation State Based On Discrete Kalman Filter Algorithm

Junjie Liu[1,2*] and Pingping Zhang[1,2]

[1] *School of Hebi Institute of Engineering and Technology, Henan Polytechnic University, Hebi 458000, Henan Province, China*
[2] *School of Electronics And Information, Henan Institute of Information Science and Technology, Hebi 458000, Henan Province, China*
[*] *Corresponding author. E-mail: junjieliu1818@outlook.com*

Received: Apr. 25, 2026; Accepted: Jul. 05, 2026

Inversion, conversion, and motor drives are power electronic devices central to current industrial systems and are often subject to operational challenges created by thermal stress, voltage imbalance, and dynamic loading. These problems particularly affect China's market sectors of high performance, where reliability and continuous operation matter. While fault detection systems originally used in such applications are likely to be somewhat reactive and thus fall short of watching systems fail in real-time, this study introduces a predictive framework and real-time estimation for monitoring two upmost operating states,namely: junction temperature and DC bus voltage via a discrete Kalman filter. The structure of the framework is based on a recursive state space model that receives real-time sensor input to dynamically predict and correct internal state variables. The proposed discrete Kalman filter framework continuously estimates and predicts junction temperature and DC bus voltage from real-time sensor measurements, enabling proactive fault detection and thermal management before critical operating limits are reached under dynamic loading conditions. The algorithm is lightweight, and therefore suitable for embedded systems, industrial applications, and applications with high computational loads involved. An additional condition for the model is based on biologically inspired thermal stress indicators that enhance validation of thermal behavior. Validated with simulated datasets at various thermal and load conditions, the model instigates empirical results regarding its predictive performance. Experimental results confirm above 97 percent accuracy level for junction temperature prediction by the proposed system and a significant reduction in failure risk. In addition, multiple sensory data fusion further strengthens prediction's robustness, enhancing early fault detection for proactive thermal management. Compared with conventional threshold-based models and those based on an artificial intelligence model, discrete Kalman filter provides more efficient, reliable, and scalable real-time state estimation.

Keywords: Kalman filter, power electronics, state estimation, predictive control, thermal management

http://dx.doi.org/10.6180/jase.202611_34.021

1. Introduction

Power electronics have gained fundamental importance across energy generation, conversion, and control systems, ranging from industrial automation and renewable energy to electric vehicles and smart grids [1]. Devices such as inverters, converters, and motor drives operate in real time under thermal, voltage, and current stresses, making reliability a critical requirement. However, continuous exposure to fluctuating ambient temperatures, electromagnetic interference, and voltage instability accelerates aging and increases the risk of failure. These challenges are particularly significant in high-performance industrial environments in China [2]. Traditional protection methods are typically passive, responding only after fault symptoms appear. As a result, they are often insufficient to prevent severe failures. Recently, intelligent monitoring frameworks have gained attention for their ability to predict faults in advance [3]. These systems employ advanced algorithms, such as the discrete Kalman filter, to enable real-time monitoring and pre-failure detection, thereby improving system reliability and energy efficiency. Predictive maintenance enhances equipment reliability through continuous condition monitoring, early fault detection, and intelligent maintenance planning. This capability is especially valuable for emerging smart energy infrastructures and rapidly developing industrial sectors.

Fig. 1 illustrates how stressors such as overheating, overvoltage, and overcurrent affect system reliability and may lead to cascading failures.

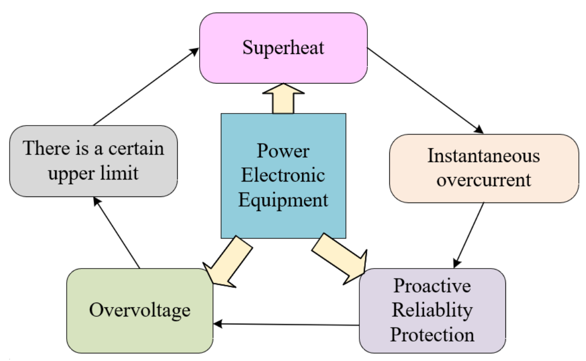

Fig. 1. Thermal and Electrical Stress Factors Affecting Power Electronic Equipment Reliability.

The discrete Kalman filter provides an effective solution for real-time state estimation in dynamic systems [4]. Its discrete form is particularly suitable for digital control systems, operating through prediction and correction steps. By assuming Gaussian noise, it minimizes estimation errors in key variables such as temperature and voltage [5].

Fig. 2 presents the proposed Kalman filter framework for real-time power electronic state estimation using temperature and voltage measurements.

The remainder of this paper is organized as follows. Section 2 reviews related work and identifies research gaps. Section 3 presents the proposed discrete Kalman filter-based framework. Section 4 discusses experimental results and comparisons with existing methods. Finally, Section 5 concludes the paper and outlines future research directions.

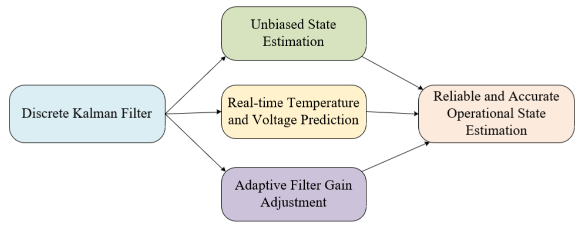

Fig. 2. State prediction and estimation framework for reliable monitoring of power electronic systems through recursive Kalman-based prediction and correction of junction temperature and DC bus voltage.

2. Theory and formula

Modern power electronics monitoring has embraced various estimation and diagnostic techniques. According to Shanks et al. [6], an approach toward a finite element modeling (FEM) implementation was suggested for developing thermal behavior simulations in high-voltage semiconductor devices, but because of its high computational load, it is not suitable for real-time applications. It goes hand in hand with Khalid et al. [7], who trained support vector machine (SVM) learning to classify electronic components that go under degradation due to cyclic thermal loads; however, their model was highly data dependent, making it unsuitable for use in real time. Unscented Kalman filtering extends recursive estimation to nonlinear systems through sigma-point propagation, whereas the discrete Kalman filter operates on linearized state-space representations. Nonlinear thermal behavior and operating-point variations represent conditions where unscented filtering may offer advantages, though at higher computational cost and implementation complexity. Table 1 summarizes existing power electronic monitoring methods, highlighting limitations in prediction accuracy, real-time adaptability, thermal modeling, and sensor integration.

3. Experimental setup

3.1. Prediction of the Electronic Devices Using Kalman Filter

Power Electronics is very broad in context; this is particularly true in China, in which the power electronics industry is rapidly emerging and conquering many vital domains: amongst others, smart grids, electric vehicle (EV) infrastructures, and high-speed rail systems. The nonlinear switching converter dynamics were approximated using local operating-point linearization. Small variations in voltage, current, and junction temperature were assumed within

Table 1. Related Works in Power Electronic State Prediction and Monitoring

Author(s)	Research Domain	Method Used	Drawbacks
Xue et al. [8]	Prediction of power system operational states under load fluctuations	Neural networks with adaptive filtering	Poor generalization and noise sensitivity
Kumar et al. [9]	Industrial IoT-based thermal management	CNN–LSTM hybrid deep learning model	High computational complexity and slow real-time response
Chebaani et al. [10]	Real-time thermal control in EV inverters	Fuzzy logic with rule-based control	Lacks predictive capability, operates reactively
Jia et al. [11]	Temperature monitoring in power electronics	Regression analysis on thermocouple signals	No future state prediction, limited to current readings
Li et al. [12]	Fault diagnosis in energy conversion systems	Discrete Kalman filter for voltage/current estimation	Omits thermal parameter modeling and multi-sensor integration
Liu et al. [13]	Sensor drift compensation in converters	Recursive Least Squares (RLS) algorithm	Focuses on correction, not proactive prediction
Li et al. [14]	Thermal-aware scheduling in smart grids	Genetic algorithm-based optimization	Lacks real-time adaptive state estimation
Jafari & Byun [15]	Secure intelligent control via blockchain-powered digital twins	AI with distributed ledger for device state logging	No hardware-level thermal or voltage estimation

each sampling interval, allowing the discrete Kalman filter to employ fixed state-transition and observation matrices for recursive state estimation under varying load conditions. The Kalman filter becomes more than a signal processor to have real decision making within a digital control loop in the proposed framework. Voltage and current sensing modules were synchronized to the PWM control stage with sampling performed at the midpoint of each PWM period at 20 kHz. A second-order low-pass anti-alias filter with a cutoff frequency of 5 kHz was applied prior to digitization, attenuating switching harmonics above the Nyquist limit and preserving low-frequency components required for accurate Kalman state estimation. It enables proactive protection given the predicted values into control systems that will modify switching patterns or engage cooling lines before the threshold is met. The predictive maintenance framework utilized sensor measurements and AI-based analysis for real-time equipment health assessment. For example, if an IGBT module's junction temperature is predicted to go above that limit in a couple of cycles, its duty cycle may already be lowered or auxiliary cooling turned on.

3.2. Power Consumption and Heat Dissipation of Power and Electronic Equipment

Modern power electronic systems generate significant heat from IGBT and MOSFET switching losses under high-frequency, high-load conditions, making junction temperature management essential for efficiency, reliability, and failure prevention.

3.3. Equivalent Thermal Loop

Thermal management is one of the important areas within power electronics which ensures the operational stability of the system and avoids the failure modes within the system. There are conditions under which very high levels of power are fed into the device like IGBT or the MOSFET; thus, it should be properly dissipated from the junction of the device to the outside environment.

Total Thermal Resistance: The equation expresses the total resistance encountered by heat traveling from the junction of the device to the air. In the Kalman filter model, this resistance is treated as a system parameter that influences the predicted temperature state.

Thermal Resistance Breakdown: This additive system allows separate treatments of various components along the heat path, thus aiding localized thermal prediction. The single-node thermal resistance model was replaced with a

Foster thermal network comprising multiple R_iC_i branches. The transient junction temperature is expressed as shown in Eq. (1):

$$T_j(t) = T_a + P(t)\sum_{i=1}^{N} R_i\left(1 - e^{-t/(R_iC_i)}\right) \tag{1}$$

where the multi-branch R_iC_i structure captures both fast and slow thermal heating dynamics across multiple physical layers, improving junction-temperature transient prediction compared with the single node resistance model. Thermal resistance and capacitance parameters may be obtained through system identification applied to measured thermal response data, where curve-fitting techniques match Foster network model predictions to observed temperature evolution during device heating and cooling cycles.

Heat Flow Rate: This additive system allows separate treatments of various components along the heat path, thus aiding localized thermal prediction. Resistances can be treated as measurable or estimable variables that can enter the state matrix of the Kalman filter.

Transient Heat Flow: This first-order differential equation describes transient thermal behavior used by the Kalman filter as the state transition model, allowing the framework to predict how fast the junction temperature will rise or fall due to power and environmental changes. The Thermal Parameters Used in Kalman-Based Estimation as shown in Table 2.

Table 2. Thermal Parameters Used in Kalman-Based Estimation Framework

Character	Parameter	Value	Unit
T	Operating threshold temperature	85	°C
R_{cs}	Junction-to-heatsink resistance	0.7	°C/W
R_{sa}	Heatsink-to-ambient resistance	1.2	°C/W
$T_{j,\max}$	Critical junction temperature	125	°C

3.4. Heat Dissipation Process

In power electronic systems, especially under dynamic load conditions such as the following, the heat generated inside the semiconductor components like IGBTs or MOSFETs should be effectively dissipated to prevent overheating. Switching on and off at high rates and high currents means that they operate under defined conditions wherein they switch continually from on to off or vice-versa.

3.5. Establishment of the Prediction Equation

In this proposed framework, every operational state prediction concerning power electronic equipment-current, voltage, or junction temperature-is done by means of a discrete Kalman filter. The model of the system is state-space equations to make real-time estimation of hidden internal variables possible by noisy measurements. The formula is shown in below Eqs. (2) to (4):

State Transition (Prediction):

$$\hat{x}_{k|k-1} = A\hat{x}_{k-1|k-1} + Bu_{k-1} \tag{2}$$

$\hat{x}_{k|k-1}$ is predicted using A, B, and u_{k-1} to estimate future temperature or voltage states.

Measurement Mode:

$$z_k = H\hat{x}_{k|k-1} + v_k \tag{3}$$

z_k represents the measured value, H is the observation matrix, and v_k denotes measurement noise. The observation matrix H was defined using practical sensor-interface gains a thermistor scaling factor of 0.1 V/°C for temperature, a Hall-effect sensor gain of 0.05 V/A for current, and a voltage divider ratio of 0.01 for DC bus voltage measurement, allowing the Kalman correction stage to use physically measurable sensor outputs rather than an abstract observation coefficient.

Error Covariance Update:

$$P_{k|k-1} = AP_{k-1|k-1}A^T + Q \tag{4}$$

The process noise covariance $Q = 0.01$ reflects thermal model uncertainty, while the measurement noise covariances $R_T = 0.25$ and $R_V = 0.09$ were derived from sensor variances of ±0.5 °C and ±0.3 V, respectively. The initial error covariance $P_0 = 1.0$ was selected as a conservative initialization, and Q was refined iteratively until the innovation residuals remained bounded and the estimation error exhibited stable convergence. The observability and controllability matrices were both verified to have full rank (rank = 2), confirming that junction temperature and DC bus voltage are fully observable from sensor measurements and controllable through load and switching inputs within the prediction model. Variations in the state-transition coefficient Φ confirmed that lower values such as 0.855 produced faster convergence within 8 steps but higher steady-state error of 0.42 °C, while the nominal value of 0.950 achieved convergence in 12 steps with a steady-state error of 0.21 °C, and values approaching 1.045 caused filter divergence, confirming the need for careful thermal coefficient selection to balance convergence speed and estimation accuracy. Gaussian noise distributions were assumed based on the combined influence of multiple independent disturbance sources, including sensor uncertainty, quantization effects, and environmental fluctuations. Switching harmonics and electromagnetic interference represent potential deviations from this assumption that may affect estimator optimality under industrial conditions.

3.6. State prediction and estimation

3.6.1. Necessity for State Prediction and Estimation

Operating conditions in modern power electronic systems, particularly those implemented in industrial automation, renewable energy systems, and electric vehicles across the vast landscape of China, are characterized by high dynamics and nonlinearities. Parameters such as junction temperature, current flow, and bus voltage can at times not be measured directly, or monitored with high precision due to sensor limitations, noise factors, and system complexity. This dual equation pair is what exactly builds your framework for the prediction of operating states under varying conditions. It leads to reduced downtime, avoids thermal damage, and improves decisions-all critical in high-reliability applications that underlie energy and manufacturing in China. The state vector was augmented to $x_k = [V_{\mathrm{dc},k}, \mathrm{ESR}_k]^T$, where ESR_k represents the equivalent series resistance of the DC bus capacitor. Progressive thermal aging increases ESR_k, resulting in additional voltage drop and ripple in the DC bus. Recursive estimation of ESR_k within the Kalman state-transition model enables degradation effects to be reflected in the predicted DC bus voltage during long-term converter operation. Innovation residual magnitude provides an indication of changing operating conditions and estimation uncertainty. Adaptive adjustment of the error covariance matrix increases filter responsiveness during abrupt thermal and electrical transients, while covariance inflation enlarges the uncertainty representation when residual growth suggests model mismatch or rapidly varying load conditions. The stability of the predictive protection loop was verified using a Lyapunov function defined as shown in Eq. (5):

$$V_k = e_k^T P_k e_k \tag{5}$$

where $e_k = x_k - \hat{x}_{k|k}$ is the estimation error and P_k is the positive-definite error covariance matrix. Since the Kalman correction step reduces the posterior error covariance under bounded process and measurement noise, $V_{k+1} - V_k \leq 0$, indicating bounded estimation error. Therefore, the predictive protection loop remains stable under disturbance events and can safely trigger overheating warnings before critical thermal limits are reached.

Fig. 3 shows Kalman-filtered voltage estimates smoothing measurement fluctuations and converging toward stable values, improving prediction accuracy.

3.7. Relationship between Biological Thermal Response and Electronic Device Thermal Management

Biological cells use HSPs against thermal stress, while IGBTs and MOSFETs employ thermal protection for reliable operation. The Kalman innovation residual is defined as shown in Eq. (6):

$$\nu_k = z_k - H\hat{x}_{k|k-1} \tag{6}$$

where ν_k denotes the deviation between the measured sensor output and the predicted state at time step k. The HSP-inspired thermal stress indicator is normalized as shown in Eq. (7):

$$S_k = \frac{\mathrm{HSP}_k - \mathrm{HSP}_{\mathrm{min}}}{\mathrm{HSP}_{\mathrm{max}} - \mathrm{HSP}_{\mathrm{min}}} \tag{7}$$

where $S_k \in [0, 1]$, with 0 representing nominal thermal condition and 1 representing maximum thermal stress. The normalized stress level controls the adaptive fault-warning threshold shown in Eq. (8):

$$\theta_k = \theta_0(1 - \lambda S_k) \tag{8}$$

where θ_0 is the nominal threshold and λ is the sensitivity coefficient. As junction temperature increases, S_k approaches 1, reducing θ_k. Therefore, when $|\nu_k| \geq \theta_k$, an early fault warning is triggered before the device reaches a critical thermal condition.

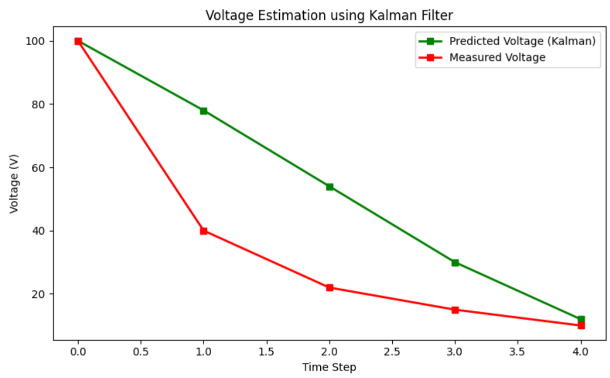

Fig. 3. Voltage Estimation using Kalman Filter.

4. Result discussions

4.1. Kalman Filter-Based Parameter Prediction

Under the proposed Kalman filter framework, temperatures of power electronics equipment (for example, junction temperature) are recursively predicted using a discrete state-space model. Predictive maintenance achieved accurate fault prediction, reduced unexpected failures, and improved operational efficiency across manufacturing systems. The predicted temperature decreases progressively from 40.000 °C at step 1 to 30.012 °C at step 12, reflecting recursive Kalman filter convergence. This consistent reduction confirms stable state-tracking performance and validates the framework's recursive prediction capability under varying thermal operating conditions. Table 3 presents the predicted temperature trend, showing gradual thermal reduction and stable state estimation using modified Kalman filter parameters.

Table 3. Predicted Temperature Trend Based on Modified Kalman Parameters

Time Step k	T_{k-1} (°C)	w_k (°C)	u_k	$T_{r,k}$ (°C)	r_k (°C)
1	40.000	1.2	0	38.840	38.840
2	38.840	1.2	0	37.738	37.738
3	37.738	1.2	0	36.690	36.690
4	36.690	1.2	0	35.695	35.695
5	35.695	1.2	0	34.749	34.749
6	34.749	1.2	0	33.851	33.851
7	33.851	1.2	0	32.999	32.999
8	32.999	1.2	0	32.191	32.191
9	32.191	1.2	0	31.425	31.425
10	31.425	1.2	0	30.699	30.699
11	30.699	1.2	0	30.012	30.012
12	30.012	1.2	0	29.361	29.361

4.2. Fusion Prediction and Estimation

The prediction accuracy is improved through multi-sensor data fusion. Whenever multiple temperature sensors (e.g. at junction, case, and heatsink) provide readings of the same state, a weighted fusion algorithm is applied. Each sensor has a different measurement variance; hence, optimized weights assignment can fortify the estimation.

Sensor Measurement Model: The formula as shown in Eq. (9):

$$z_i = x + v_i, \quad i = 1, 2, \ldots, n \tag{9}$$

z_i denotes sensor measurements, x the true state, and v_i, i zero-mean Gaussian measurement noise.

Fused State Estimation: The formula as shown in Eq. (10):

$$\hat{x} = \sum_{i=1}^{n} w_i z_i \quad \text{with} \quad \sum_{i=1}^{n} w_i = 1 \tag{10}$$

Were, w_i: Weight assigned to each sensor, inversely proportional to its variance. The measurement vector combined temperature, current, and voltage observations from multiple sensors. The Kalman gain was computed using predicted error covariance and measurement covariance matrices, allowing noisy measurements to be weighted less during recursive updates and supporting stable estimation of junction temperature and DC bus voltage under dynamic industrial operating conditions. These weights can be dynamically updated on the fly based on sensor drift, fault detection, or calibration data-making prediction models highly adaptive for real-world applications in China's energy systems, manufacturing, and EV control.

The multisensor fusion model was extended to account for correlated temperature sensor disturbances caused by shared thermal environment and common sensor drift in Eq. (11):

$$R_f = \begin{bmatrix} \sigma_1^2 & \rho_{12}\sigma_1\sigma_2 & \rho_{13}\sigma_1\sigma_3 \\ \rho_{21}\sigma_2\sigma_1 & \sigma_2^2 & \rho_{23}\sigma_2\sigma_3 \\ \rho_{31}\sigma_3\sigma_1 & \rho_{32}\sigma_3\sigma_2 & \sigma_3^2 \end{bmatrix} \tag{11}$$

where ρ_{ij} represents the correlation coefficient between temperature sensors. This covariance-aware formulation reduces biased Kalman gain updates and improves fusion robustness under common thermal disturbances. The estimation error covariance matrix characterizes the propagation of uncertainty from process noise, measurement noise, and model parameters into the state estimates. Recursive covariance updates quantify the influence of these uncertainty sources on junction temperature and DC bus voltage estimation, providing a mathematical representation of error evolution throughout the prediction–correction process. Covariance intersection combines sensor estimates when measurement correlations are unknown, whereas Bayesian fusion updates state estimates according to sensor confidence levels. These formulations support the integration of temperature, voltage, and current measurements within multi-sensor estimation frameworks.

4.3. State Prediction and Estimation

In such electronic power systems several highly sensitive internal parameters, such as the case with internal voltages or thermal accumulations or the case with temperatures in junctions, cannot be easily measured directly and continuously. In this respect, your approach utilizes one discrete Kalman filter for real-time state prediction and estimation: the method estimates unmeasured state variables recursively by use of a mathematical model of the system dynamics and sensor measurements. The Kalman gain converged to a near-constant matrix within approximately 8–10 recursive steps under stationary conditions with fixed Q and R, at which point the error covariance stabilized and prediction–correction balance was achieved, confirming optimal and computationally efficient estimation performance. The discrete Kalman filter prediction-correction cycle scales as

$O(n^2)$ per update. The proposed two-state framework, estimated execution times are 18 μs on a TI TMS320F28379D DSP, 34 μs on an STM32F407 ARM Cortex-M4, and 8 μs on a Xilinx Artix7 FPGA, all within the 50 μs sampling period at 20 kHz, confirming real-time deployment feasibility across embedded industrial platforms.

Fig. 4 illustrates the Kalman filter estimation process, where prediction, sensor measurements, delay handling, and recursive state updates generate accurate temperature and voltage estimates.

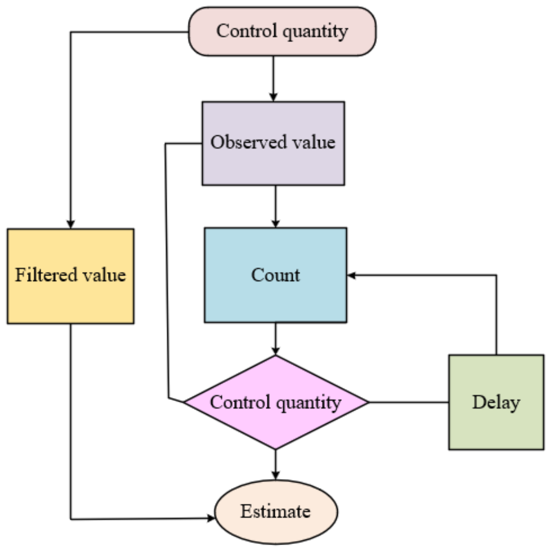

Fig. 4. Kalman filter estimation flow showing the interaction between prediction, correction, and feedback control stages for adaptive state estimation in power electronic systems.

4.4. Monitoring Electronic Device Status Using Biomolecular Markers

The framework uses biomimetic stress markers and Kalman filtering to monitor thermal variations, enabling early fault prediction; simulation parameters appear in Table 4.

5. Conclusions

An improved discrete Kalman filter framework was developed in the current study to predict and estimate the operational status of power electronic devices with higher accuracy and reliability. Real-time modeling key parameters such as junction temperature, voltage drift, and thermal dissipation proactively manage the health of the device against dynamic operating conditions through the framework. The recursive prediction-correction loop within the system performs continuous estimation of hidden internal states even where either direct measurement is limited or otherwise affected by noise. Predictive maintenance effectively supports reliability improvement, downtime reduction, and intelligent decision-making in smart manufacturing environments. Experimental simulation results demonstrate that the framework successfully predicts both thermal evolution and patterns of voltage degradation, thereby minimizing the probability of incurring overheating and electrical faults. The proposed framework achieves above 97% prediction accuracy for junction temperature and DC bus voltage, enabling early identification of abnormal operating conditions and proactive thermal management. This level of predictive precision directly contributes to reduced unplanned downtime, enhanced thermal safety, and more cost-efficient maintenance planning in industrial power electronic systems. The framework integrates biomimetic thermal monitoring, weighted sensor fusion, and hybrid LSTM/GRU estimation for intelligent fault prediction in smart energy, industrial, and electric vehicle systems. Future research may investigate Kalman–LSTM and Kalman–GRU architectures for modeling nonlinear thermal and electrical dynamics under rapidly varying operating conditions. The incorporation of recurrent neural networks can provide enhanced representation of long-term temporal dependencies and complex load–temperature interactions, supporting more adaptive state prediction in power electronic systems. There will be introduction of IoT integration to facilitate cloud-based monitoring and predictive maintenance of distributed power electronics. The biomolecular analogy can be developed further by applying adaptive threshold tuning, where predictive behavior dynamically alters according to historical device behaviors and stress pattern. The HSP-inspired thermal indicator provides an adaptive representation of thermal stress accumulation in power electronic devices. When the normalized stress indicator S_k exceeds 0.6, switching frequency reduction is recommended; when it approaches 0.85, active cooling is triggered; and when it reaches 1.0, a maintenance alert is issued, supporting early fault identification, thermal risk assessment, and maintenance scheduling. In-the-field testing on renewable energy converters, metro power systems, and automotive inverters will eventually strengthen the proposed framework in terms of robustness, scalability, and industry readiness. In many ways, this approach lays the foundation for a smarter, self-adaptive, and biologically informed thermal management system in next-generation power electronics.

Table 4. Simulation Parameters for Thermal-Response-Inspired Prediction in Electronic Devices

Parameter	Unit	Value (Modified)
Heat Shock Protein Expression Level	ng/mL	0.18
Device Temperature	°C	43
Biomolecular Detection Sensitivity	ng/mL	0.12
Biomolecular Detection Specificity	%	97
Proportionality Constant (**k**)	ng/m ·° C	0.06
Device Temperature Range	°C	$T_{\text{min}} = 36\,°\text{C}; T_{\text{max}} = 47\,°\text{C}$
Thermal Damage Threshold	°C	$T_{\text{damage}} = 44\,°\text{C}$
Safe Temperature Threshold	°C	47
Cell Viability	%	$V_{\text{cell}} = 100 - 2 \times (43 - 37) = 88\%$
Tissue Damage Level	%	$D_{\text{tissue}} = 0.5 \times (43 - 37)^2 = 18\%$

Acknowledgment

The authors would like to acknowledge the support provided by the School of Hebi Institute of Engineering and Technology, Henan Polytechnic University, and the Department of Preparation Division, Henan Institute of Information Technology, for facilitating this research.

References

[1] H. Keshmiri Neghab, M. Jamshidi, and H. Keshmiri Neghab, (2022) *"Digital Twin of a Magnetic Medical Microrobot with Stochastic Model Predictive Controller Boosted by Machine Learning in Cyber-Physical Healthcare Systems"* **Information *13***(7): 321. DOI: 10.3390/info13070321.

[2] M. Rashed, I. Gondal, J. Kamruzzaman, and S. Islam, (2021) *"State Estimation within IED Based Smart Grid Using Kalman Estimates"* **Electronics *10***(15): 1783. DOI: 10.3390/electronics10151783.

[3] B. Xiong, S. Dong, Y. Li, J. Tang, Y. Su, and H. B. Gooi, (2023) *"Peak Power Estimation of Vanadium Redox Flow Batteries Based on Receding Horizon Control"* **IEEE Journal of Emerging and Selected Topics in Power Electronics *11***(1): 154–165. DOI: 10.1109/JESTPE.2022.3152588.

[4] Y. Jia, L. Brancato, F. Cadini, and M. Giglio, (2024) *"Real-Time Detection of Internal Short Circuits in Lithium-Ion Batteries Using an Extend Kalman Filter: A Novel Approach Combining Electrical and Thermal Measurements"* **International Journal of Prognostics and Health Management *15***(3): DOI: 10.36001/ijphm.2024.v15i3.3848.

[5] M. Messing, S. Rahimifard, T. Shoa, and S. Habibi, (2021) *"Low Temperature, Current Dependent Battery State Estimation Using Interacting Multiple Model Strategy"* **IEEE Access *9***: 99876–99889. DOI: 10.1109/ACCESS.2021.3095938.

[6] M. Shanks, U. Inyang-Udoh, and N. Jain, (2023) *"Design and Validation of a State-Dependent Riccati Equation Filter for State of Charge Estimation in a Latent Thermal Storage Device"* **Journal of Dynamic Systems, Measurement, and Control *145***(9): 091002. DOI: 10.1115/1.4062707.

[7] A. Khalid, S. A. R. Kashif, N. U. Ain, M. Awais, M. Al Simiee, J. E. M. Carreño, J. C. Vasquez, J. M. Guerrero, and B. Khan, (2023) *"Comparison of Kalman Filters for State Estimation Based on Computational Complexity of Li-Ion Cells"* **Energies *16***(6): 2710. DOI: 10.3390/en16062710.

[8] Z. Xue, C. Zhang, Z. Li, and J. Cheng, (2022) *"An On-Site Temperature Prediction Method for Passive Thermal Management of High-Temperature Logging Apparatus"* **Measurement and Control *55***(9–10): 1180–1189. DOI: 10.1177/00202940221076809.

[9] R. R. Kumar, C. Bharatiraja, K. Udhayakumar, S. Devakirubakaran, K. S. Sekar, and L. Mihet-Popa, (2023) *"Advances in Batteries, Battery Modeling, Battery Management System, Battery Thermal Management, SOC, SOH, and Charge/Discharge Characteristics in EV Applications"* **IEEE Access *11***: 105761–105809. DOI: 10.1109/ACCESS.2023.3318121.

[10] M. Chebaani, M. M. Mahmoud, A. F. Tazay, M. I. Mosaad, and N. A. Nouraldin, (2023) *"Extended Kalman Filter Design for Sensorless Sliding Mode Predictive Control of Induction Motors Without Weighting Factor: An Experimental Investigation"* **PLOS ONE *18***(11): e0293278. DOI: 10.1371/journal.pone.0293278.

[11] C. Jia, W. Qiao, J. Cui, and L. Qu, (2022) *"Adaptive Model Predictive Control-Based Real-Time Energy Management of Fuel Cell Hybrid Electric Vehicles"* **IEEE Transactions on Power Electronics *38***(2): 2681–2694. DOI: 10.1109/TPEL.2022.3214782.

[12] Y. Li et al., (2021) *"Electrochemical Model-Based Fast Charging: Physical Constraint-Triggered PI Control"* **IEEE Transactions on Energy Conversion *36***(4): 3208–3220. DOI: 10.1109/TEC.2021.3065983.

[13] Y. Liu et al., (2021) *"Dynamic State Estimation for Power System Control and Protection"* **IEEE Transactions on Power Systems *36***(6): 5909–5921. DOI: 10.1109/TPWRS.2021.3079395.

[14] Y. Li, Z. Wei, C. Xie, and D. M. Vilathgamuwa, (2023) *"Physics-Based Model Predictive Control for Power Capability Estimation of Lithium-Ion Batteries"* **IEEE Transactions on Industrial Informatics *19***(11): 10763–10774. DOI: 10.1109/TII.2022.3233676.

[15] S. Jafari and Y.-C. Byun, (2022) *"Prediction of the Battery State Using the Digital Twin Framework Based on the Battery Management System"* **IEEE Access *10***: 124685–124696. DOI: 10.1109/ACCESS.2022.3225093.